PERGAMON

Control Engineering Practice 10 (2002) 685–696

CONTROL ENGINEERING PRACTICE

www.elsevier.com/locate/conengprac

Scheduling schemes for an integrated flight and propulsion control system ☆

Nabil Aouf[a], Declan G. Bates[b,*], Ian Postlethwaite[b], Benoit Boulet[a]

[a] Department of Electrical and Computer Engineering, McGill University, Montreal, Canada

[b] Control and Instrumentation Research Group, Department of Engineering, University of Leicester, University Road, Leicester LE1 7RH, UK

Received 21 June 2001; accepted 14 December 2001

Abstract

We describe two schemes for scheduling an integrated flight and propulsion control system for an experimental vertical/short take-off and landing (V/STOL) aircraft concept in the acceleration from hover (0–120 kn) flight phase. Multivariable integrated flight and propulsion controllers are designed at several points over the V/STOL envelope and implemented as exact plant observers with state feedback. In the first scheduling scheme, the values of the state feedback and observer gain matrices are interpolated between the fixed-point designs as a function of aircraft speed. In the second approach, the control signals produced by the different fixed-point controllers are blended, allowing a significant reduction in the order of the scheduled controllers. Both scheduling schemes are shown in non-linear simulation to provide excellent handling qualities as the aircraft accelerates from the hover.

Keywords: Aerospace; Robust; Flight; Engine control

1. Introduction

Research into the design of integrated flight and propulsion control (IFPC) systems (Garg, 1993a, b) is motivated by the desire to exploit potentially significant gains, both in terms of improved flying qualities and reduced pilot workload, which may be obtained by the use of propulsive system generated forces and moments for aircraft manoeuvring in the low-speed region of the flight envelope. Recent advances in aerospace actuator technologies allow a significant amount of 'extra' control power to be generated via, for example, thrust vectoring and reversing nozzles, reaction control systems, air blowing/sucking devices, etc. While the most obvious current application of these new technologies is in the area of super-manoeuvrable vertical/short take-off and landing (V/STOL) fighter aircraft (Wise, 1995), research into control technology requirements for future supersonic transport aircraft and hypersonic aerospacecraft has also indicated the necessity of fully integrating the airframe and engine control systems (Steer, 2000; Schmidt, 1993).

In Bates, Gatley, Postlethwaite, and Berry (1999), a robust integrated flight and propulsion controller was designed for an experimental V/STOL aircraft configuration, using the method of $\mathscr{H}_\infty$ loopshaping. The aircraft simulation model used in the study has been developed by Qinetiq (formerly the UK Defence and Evaluation Research Agency (DERA)) to explore issues associated with the integration of airframe and engine control systems for future V/STOL aircraft. Results of piloted simulation trials with this centralised IFPC system are reported in Bates, Gatley, Postlethwaite, and Berry (2000). The IFPC system examined in these trials was designed at the 80 kn point of the V/STOL flight envelope, where control of the aircraft is starting to pass from purely propulsion system effectors (thrust vectoring nozzles, etc.) to conventional aerodynamic control surfaces. These trials examined the handling qualities of the IFPC system over a range of speeds from 50 to 110 kn. While the single controller was found to deliver level 1 handling qualities on the Cooper–Harper scale

☆ This work was performed while the first author was a visiting researcher in the Department of Engineering at the University of Leicester.

*Corresponding author. Tel.: +44-0116-252-5642; fax: +44-0116-252-2619.

E-mail address: dgb3@le.ac.uk (D.G. Bates).

0967-0661/02/$ - see front matter
PII: S0967-0661(02)00028-X

Nomenclature

IFPC	integrated flight and propulsion control
V/STOL	vertical/short take-off and landing
RTAVS	real time all vehicle simulator
DERA	Defence and Evaluation Research Agency
WEM	wide envelope model
VAAC	vectored thrust aircraft advanced flight control
HUD	head up display
γ	flight path angle (deg)
α	aircraft angle of incidence (deg)
$\dot{\gamma}$	flight path angle rate (deg/s)
θ	pitch angle (deg)
VT	velocity along the flight path (kn)
THM	thrust magnitude (kN)
THD	thrust direction (deg)
NLPC	low-pressure compressor spool speed (%)
*T*10	high-pressure turbine stator outlet temperature (K)
HPSM	high-pressure compressor surge margin (%)
LPSM	low-pressure compressor surge margin (%)
ETAD	elevator position (-15° to $+15^\circ$)
ETASTK	pitch reaction control system position (-15° to $+15^\circ$)
FNOZ	front nozzle position (-5° to $+120^\circ$)
RNOZ	rear nozzle position (-5° to $+120^\circ$)
SPLIT	engine thrust split (0−1:0 = all to front, 1 = all to rear)
MFF	main fuel flow (0–1.2 kg/s)
ENOZA	exit nozzle area (0.8307–0.1602 sine petal angle)
IGV	inlet guide vane angle (-8° to $+35^\circ$)
RCS	reaction control system

(Cooper & Harper, 1969), at speeds close to its design point, performance was seen to degrade to level 2 quality as the aircraft moved further away from the 80 kn point of the flight envelope. This degradation in performance is caused by the large changes in both aerodynamics and engine dynamics typically exhibited by V/STOL aircraft in acceleration from hover to fully wingborne flight.

In this paper we describe the design of two different scheduling schemes for the IFPC system which maintain level 1 type handling qualities as the aircraft accelerates from hover to 120 kn, while also keeping the specified engine variables within their safety limits. The first scheme used (also discussed in Aouf, Bates, & Postlethwaite, 2001) is similar to that developed and flight tested in Hyde (1995), on the DERA VAAC Harrier, and exploits a particular property of $\mathscr{H}_\infty$ loopshaping controllers which allows them to be written as exact plant observers with state feedback. Note, however, that the system tested in Hyde (1995) considered only the control of airframe states, and implemented traditional Harrier control modes, i.e. left-hand inceptor (throttle lever) controls a blend of forward acceleration and forward speed, right-hand inceptor (centre stick) controls vertical acceleration at low speeds and pitch rate in normal flight, and a trim switch on the stick controls pitch attitude at low speeds. The IFPC system discussed in this paper is required to directly control several engine variables, and implements a two-inceptor control mode where the centre stick controls the flight path angle rate $\dot{\gamma}$ and the throttle lever commands velocity along the flight path.

The second approach described in this paper is a version of the blending/interpolating technique implemented successfully for a missile application in Buschek (1999). In this scheme the output signals of two controllers were interpolated in a local region near the second controller, and a conditioning scheme was applied to smooth the transition in the interpolation region. The approach adopted here is different, in that the controller signals are continuously interpolated as a function of speed with the result that no 'bumpless transfer' type conditioning is required.

Both of the schemes described in this paper are quite similar to classical approaches for gain scheduling of single-loop flight control laws, in that individual controllers are designed over a set of points in the envelope and these controllers are then 'stitched' together using some form of blending or interpolation. An alternative to this philosophy is provided by the recently developed linear parameter varying (LPV) control techniques (Shamma & Cloutier, 1993; Papageorgiou, Glover, D'Mello, & Patel, 2000), which offer the potential to directly design controllers with guaranteed stability properties over the full flight envelope. In order to use these techniques, however, a quasi-LPV model of the plant dynamics must first be developed (see the work reported in Papageorgiou and Glover (2000) on developing such a model for the standard Harrier aircraft), and computationally intensive LMI-based optimisation problems must be solved to calculate the controller. For the V/STOL aircraft configuration considered in this paper, both of these requirements are problematic—the nature of the aircraft model (interacting engine and airframe sub-models, developed independently and subsequently integrated) makes accurate LPV models very difficult to

construct, and the high order of the overall system makes LMI-based optimisation computationally expensive.

The paper is organised as follows. Section 2 describes the aircraft simulation model used in the study and summarises the specifications for the IFPC system. In Section 3, the procedure used to design $\mathscr{H}_\infty$ loopshaping controllers at several operating points over the low-speed flight envelope is described. The two controller scheduling schemes are described in Sections 4 and 5. Section 6 presents some conclusions.

2. Aircraft model and IFPC system specifications

The airframe model used in this study is based on the non-linear DERA Bedford Harrier T.Mk4 Wide Envelope Model (WEM), which been used extensively in the VAAC Harrier research program (Tischler, 1996), and has been established through flight trials as being representative of the real aircraft. The original Pegasus engine previously included in the WEM has been replaced with a high-fidelity thermodynamic model of a Rolls Royce Spey engine. The Spey is a two-spool reheated turbofan engine with the same basic architecture, for the purposes of control, as the EJ200, which is used to power the Eurofighter. This engine model allows the control law designer full access to engine actuators such as inlet guide vane angle, fuel flow rate and exit nozzle area. The engine thrust is vectored through four nozzles similar to the standard Harrier. Total thrust and high-pressure bleed flow to the reaction control system (RCS) are scaled to match Pegasus performance and no duct losses are modelled in the rotating nozzles. The effect of high-pressure bleed flow (to the RCS) on the engine operating point is modelled, and the effect of front/rear thrust split on engine performance is assumed to be negligible.

To increase the design difficulty, and to more closely represent likely future V/STOL aircraft configurations, the front pair of nozzles has been moved forward and downward to displace the centre of thrust from the centre of gravity and introduce thrust/pitching moment interactions. Also, unlike with the standard Harrier, the thrusts from front and rear nozzle pairs can be modulated and vectored independently. Finally, representative non-linear actuation systems including both rate and magnitude limits (as well as deadzones and hysteresis for the thrust-vectoring nozzles) have been placed on all control motivators. The model offers a six degree of freedom non-linear simulation over a flight envelope from -20 to 250 kn, and includes automated routines for trimming and linearising the aircraft over the flight envelope.

The results presented in this paper relate to the control of the longitudinal axis only, and the control law is required to follow a two-inceptor strategy. Functional specifications for the IFPC system are given as follows:

(a) *Flight path manoeuvre demand*: The right-hand pitch control law will command flight path angle rate and should actively hold flight path with the stick centred. Stick displacement will produce a flight path rate demand up to a maximum of $3.0^\circ/\mathrm{s}$. A maximum transient speed change of ± 2 kn during any flight path manoeuvre is desirable.

(b) *Velocity demand*: Left-hand inceptor displacement will demand velocity parallel to flight path (VT). A maximum transient deviation of $\pm 0.3^\circ$ in the flight path angle is desirable during velocity changes of up to ± 30 kn.

(c) *Incidence limit*: To avoid extreme incidence angles, which can lead to lateral/directional instability, an incidence boundary is necessary. The aircraft angle of incidence, α, should therefore be kept within $+12.0^\circ$ and -6.0° during all manoeuvres.

(d) *Engine safety limits*: To protect engine components from dangerous over stress and over temperature, and to ensure avoidance of surge conditions, the following set of engine limits are to be respected during all manoeuvres:

(1) low-pressure compressor spool speed $(NLPC) < 102\%$;
(2) high-pressure turbine stator outlet temperature $(T10) < 1430$ K;
(3) high-pressure compressor surge margin $(HPSM) > 10\%$;
(4) low-pressure compressor surge margin $(LPSM) > 10\%$.

Recommended maximum limits were also provided for five other engine variables—see Bates et al. (2000) for details.

3. Centralised IFPC system design

Since this paper is mainly concerned with the design and implementation of scheduling schemes for the IFPC system, we give only a brief outline of the $\mathscr{H}_\infty$ loopshaping technique used to design the individual controllers. More details on the design of the IFPC system at the 80 kn operating point are available in Bates et al. (1999), while a comprehensive tutorial on the $\mathscr{H}_\infty$ loopshaping design method is given in Papageorgiou and Glover (1999). The controllers were designed for linearised models of the aircraft/engine dynamics, generated at the 0, 20, 50, 80 and 120 kn points of the flight envelope. The resulting state space models of the

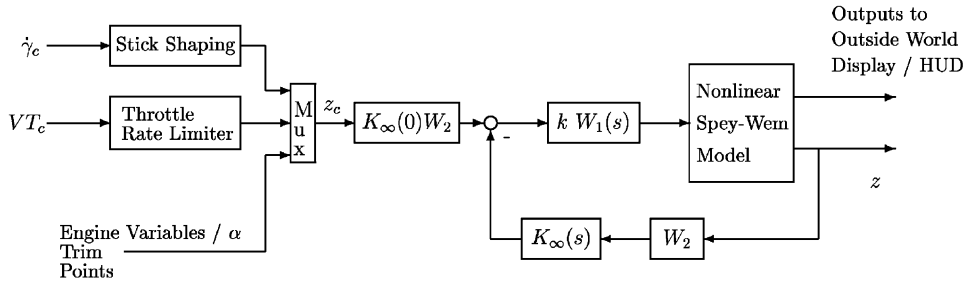

Fig. 1. Controller implementation structure for piloted simulation trial.

integrated airframe and engine systems, plus actuators, have 35 states and are of the form

$$\dot{x} = Ax + Bu, \quad y = Cx + Du.$$

The control inputs are given by

$$u = [ETAD, ETASTK, FNOZ, RNOZ, SPLIT, MFF, ENOZA, IGV],$$

while the vector of outputs y includes eight airframe and 19 engine variables. Based on the performance requirements previously detailed, the vector of controlled variables z was chosen as

$$z = [\alpha, VT, \dot{\gamma}, NLPC, T10, HPSM, LPSM].$$

The angle of incidence α was included in z in order to explicitly minimise deviations from its trim point during manoeuvres.

The $\mathscr{H}_\infty$ loopshaping design method used to design the controllers (McFarlane & Glover, 1992) is essentially a two-stage process. First, the open-loop plant is augmented by (generally diagonal) weighting matrices to give a desired shape to the singular values of the open-loop frequency response. Then, the resulting shaped plant is robustly stabilised with respect to coprime factor uncertainty using $\mathscr{H}_\infty$ optimisation. The implementation structure for the $\mathscr{H}_\infty$ loopshaping controller used in the piloted simulation trial is shown in Fig. 1. With reference to this figure, the weighting matrix $W_1(s)$ is chosen to add integral action and ensure reasonable roll-off rates for the open-loop singular values around the desired crossover frequencies. The constant weighting matrix k is then used to adjust control actuation requirements with respect to the various actuator rate and magnitude limits. Note that in this configuration the non-linear Spey-Wem aircraft model is scaled so as to be approximately normalised with respect to maximum allowable input signals. The constant matrix W_2 is used to prioritise airframe-controlled variables (which must achieve specific handling qualities characteristics) over engine variables (which have simply to be limited within certain values). For the 80 kn controller

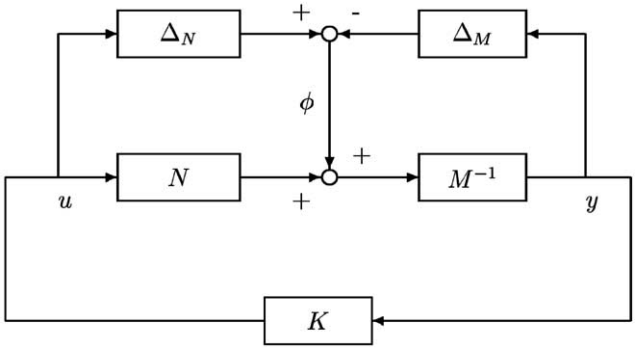

Fig. 2. Normalised coprime factor uncertainty description.

for example, the three weighting matrices were chosen as

$$k = \mathrm{diag}(0.13, 0.1, 0.25, 0.25, 0.25, 0.2, 0.2, 0.2),$$

$$W_1 = \frac{s+2}{s} \times I_{8\times 8},$$

$$W_2 = \mathrm{diag}(1, 1, 1, 1/200, 1/800, 1/200, 1/500).$$

The second stage of the $\mathscr{H}_\infty$ loopshaping design method involves the use of $\mathscr{H}_\infty$ optimisation to compute a controller block K_∞ which robustly stabilises the shaped plant against a particular type of uncertainty description, based on stable perturbations to each of the factors in a normalised coprime factorisation of the plant. For a plant G with a normalised left coprime factorisation (Skogestad & Postlethwaite, 1996),

$$G_s = M^{-1}N. \tag{1}$$

An uncertain plant model G_p can then be written as

$$G_p = (M + \Delta_M)^{-1}(N + \Delta_N), \tag{2}$$

where Δ_M and Δ_N are stable unknown transfer function matrices which represent the uncertainty in the nominal plant model G—see Fig. 2. The objective of robust stabilisation is to stabilise the class of perturbed plants defined by

$$G_p = \{(M + \Delta_M)^{-1}(N + \Delta_N): \|[\Delta_N\ \Delta_M]\|_\infty < \varepsilon\}, \tag{3}$$

where ε is the stability margin. Note that ε also has an interpretation in terms of classical gain and phase margin specifications (Glover, Vinnicombe, & Papageorgiou, 2000). Now, as shown in McFarlane and Glover (1992), the largest possible class of such systems, i.e. the maximum of ε, $\varepsilon_{\max}$, is given by

$$\gamma_{min} = \inf_K \left\| \begin{bmatrix} K \\ I \end{bmatrix} (I - G_s K)^{-1} M^{-1} \right\|_\infty = \frac{1}{\varepsilon_{max}}. \tag{4}$$

Note that γ_{min} is the minimum over all stabilising controllers of the $\mathscr{H}_\infty$ norm from ϕ to $\begin{bmatrix} u \\ y \end{bmatrix}$ in Fig. 2. The solution of the above equation is particularly attractive in that γ_{min} can be calculated, using readily available commerical software, without recourse to the γ-iteration which is normally required to solve $\mathscr{H}_\infty$ control problems. Given a minimal realisation $[A_s, B_s, C_s, D_s]$ of a controllable and observable shaped plant G_s, the solutions X_s and Z_s of the two Riccati equations:

$$A_z Z_s + Z_s A_z^* - Z_s C_s^* R^{-1} C_s Z_s + B_s S^{-1} B_s^* = 0, \tag{5}$$

$$A_z^* X_s + X_s A_z - X_s B_s S^{-1} B_s^* X_s + C_s^* R^{-1} C_s = 0, \tag{6}$$

where

$$A_z = A_s - B_s S^{-1} D_s^* C_s,$$

$$R = I + D_s D_s^*, \quad S = I + D_s^* D_s,$$

give the optimal γ,

$$\gamma_{min} = \{1 - \|[N \quad M]\|_H^2\}^{-1/2} = (1 + \rho(X_s Z_s))^{1/2}, \tag{7}$$

where $\|.\|_H$ denotes the Hankel norm and ρ denotes the spectral radius. The so-called central controller K_∞ which guarantees that

$$\left\| \begin{bmatrix} K \\ I \end{bmatrix} (I - G_s K)^{-1} M^{-1} \right\|_\infty \leqslant \gamma \tag{8}$$

for a specified $\gamma > \gamma_{min}$, is then given by

$$K_\infty = \left[\begin{array}{c|c} A_k & B_k \\ \hline C_k & D_k \end{array} \right] \tag{9}$$

with

$$A_k = A_s + B_s F + \gamma^2 (L^*)^{-1} Z_s C_s^* (C_s + D_s F), \tag{10}$$

$$B_k = \gamma^2 (L^*)^{-1} Z C_s^*, \tag{11}$$

$$C_k = B_s^* X, \tag{12}$$

$$D_k = -D_s^*, \tag{13}$$

where

$$F = -S^{-1}(D_s^* C_s + B_s^* X_s), \tag{14}$$

$$L = (1 - \gamma^2) I + X_s Z_s. \tag{15}$$

For $\gamma < 4$ (i.e. an allowable coprime factor uncertainty of $> 25\%$) it can be shown theoretically (McFarlane & Glover, 1992), that the controller $K_\infty(s)$ does not significantly change the shapes of the open-loop singular values. Thus robust stability is achieved without significant degradation in performance characteristics. If $\gamma > 4$, this indicates that the chosen loop shapes are incompatible with robust stability, and further adjustments of the weighting functions are then required. The final step of the design procedure is to add the constant prefilter $K_\infty(0) W_2$ in order to ensure zero steady-state tracking error, assuming integral action in W_1. The K_∞ controller block for each operating point is of order equal to that of the shaped plant, i.e. for each of our designs, K_∞ has 43 states.

4. Observer-form implementation and scheduling

In Sefton and Glover (1990), it was shown that the controller resulting from the $\mathscr{H}_\infty$ loopshaping procedure can be written as an exact observer for the shaped plant plus state feedback. Assuming, purely for notational convenience, a strictly proper shaped plant, with a stabilisable and detectable state-space realisation

$$G_s = \left[\begin{array}{c|c} A_s & B_s \\ \hline C_s & 0 \end{array} \right], \tag{16}$$

the relevant equations for the observer and state-feedback controller matrices are

$$\dot{\hat{x}}_s = A_s \hat{x}_s + H_s(C_s \hat{x}_s - y_s) + B_s u_s, \tag{17}$$

$$u_s = K_s \hat{x}_s, \tag{18}$$

where $\hat{x}_s$ is the observer state, u_s and y_s are, respectively, the input and output of the shaped plant, and

$$H_s = -Z_s C_s^*, \tag{19}$$

$$K_s = -B_s^* [I - \gamma^{-2} I - \gamma^{-2} X_s Z_s]^{-1} X_s, \tag{20}$$

where Z_s and X_s are the appropriate solutions to the generalised algebraic Riccati equations for G_s given in (5) and (6). In general, $\mathscr{H}_\infty$ controllers cannot be written as exact plant state observers, as there will be a worst-case disturbance term entering the observer state equation (Doyle, Glover, Khargoneker, & Francis, 1989). However, for the controllers produced by the $\mathscr{H}_\infty$ loopshaping method it is possible, and this clear structure lends itself to gain scheduling in that the observer and controller matrices H_s and K_s can be simply scheduled as a function of one or more aircraft parameters. Fig. 3 shows the implementation structure of the IFPC system scheduled as a function of aircraft speed. Note that the observer is for the shaped plant G_s, and thus this places some limitations on the choice of the weighting functions for each of the linear controller designs, i.e. they must have a fixed structure. Otherwise,

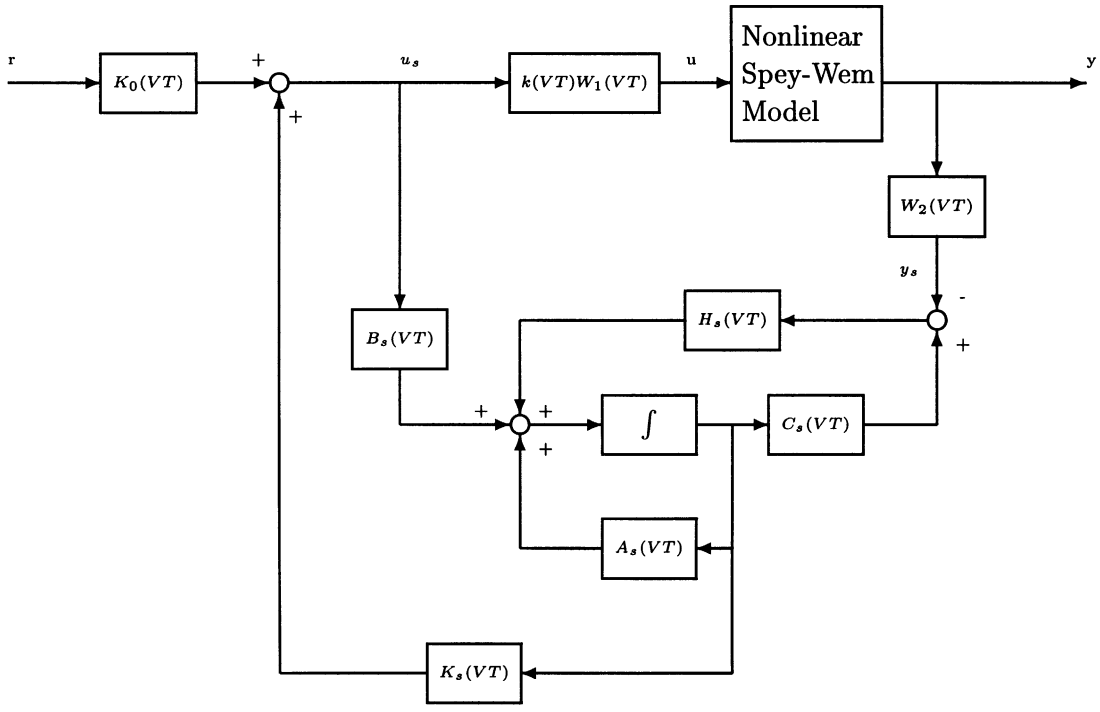

Fig. 3. Observer-form implementation for controller scheduling.

from an implementation point of view, there is little difference between $\mathscr{H}_\infty$ loopshaping controllers written in this form and the classical LQG/LTR structure of modern control theory (Stevens & Lewis, 1992).

For each of the linear designs between 0 and 120 kn, the weighting function $W_1(s)$ was thus chosen to be of the form

$$W_1(s) = \frac{s+a}{s}$$

with the parameter a varying smoothly between different design points. For successful operation of the scheduled system, it is desirable that the observer and controller gains H_s and K_s vary smoothly with operating point. A theorem in Ran and Rodman (1988) can be used to show that this condition will be satisfied provided the Riccati solutions X_s and Z_s and the stability margin γ vary smoothly. Another condition for successful implementation of the scheduled system is that the shaped plant matrices A_s, B_s, C_s vary smoothly with operating point, while also capturing the important changes in the dynamics of the plant over the specified portion of the envelope—knowledge of the aircraft and engine dynamics needs to be used here to decide on the position and number of design points required for interpolation. Some extra freedom can also be introduced by using a weighting function VT^p in the interpolation of the different matrices,

$$A_s(VT) = (1 - VT^p)A_{si} + VT^p\, A_{sj}$$

so that the power p can be adjusted to get a better match between the interpolated linear system matrices and the actual non-linear system. Note that the constant prefilter must be recalculated at each operating point to take account of the different structure of the observer-form implementation. Since we now have that

$$y = -(I + TH_sW_2)^{-1}(TB_s + GW_1k)r \tag{21}$$

with

$$T = GW_1kK_s(sI - A_s - H_sC_s - B_sK_s)^{-1}, \tag{22}$$

in order to have zero steady-state error, we choose a constant prefilter K_0 given by

$$K_0 = -(TB_s + GW_1k)^{-1}(I + TH_sW_2)|_{s=0}. \tag{23}$$

Assuming integral action in W_1, this simplifies to

$$K_0 = (I + RB_s)^{-1}(-RH_sW_2), \tag{24}$$

where

$$R = -K_s(A_s + H_sC_s + B_sK_s)^{-1}.$$

This constant prefilter must then also be scheduled as a function of speed in order to take account of variations in the low-frequency gain of the controller over the envelope.

Non-linear simulation results for the scheduled IFPC system in the acceleration from hover phase are shown in Figs. 4–6. The figures show close tracking of velocity demands as the aircraft accelerates from 0 to 120 kn, with only small deviations in flight path angle during the manoeuvre. In addition, the four directly controlled engine variables are kept within their specified safety limits (see Fig. 6), and α is regulated close to its nominal value throughout (see Fig. 4). The necessity for a gain-scheduling scheme to preserve performance throughout this portion of the flight envelope is demonstrated in Figs. 7 and 8, which compare the performance of the

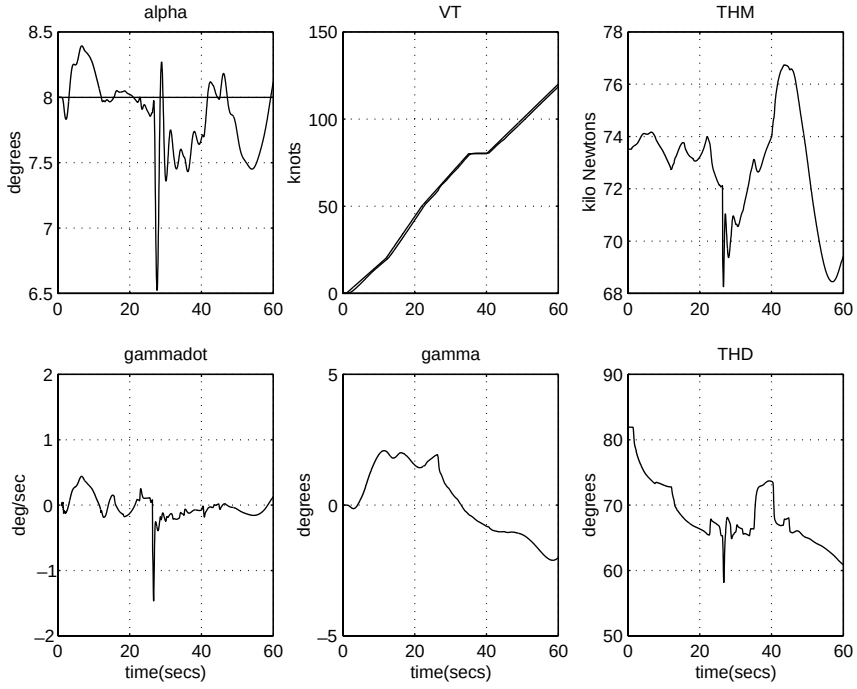

Fig. 4. Response of scheduled IFPC system for pilot demands on VT in the acceleration hover.

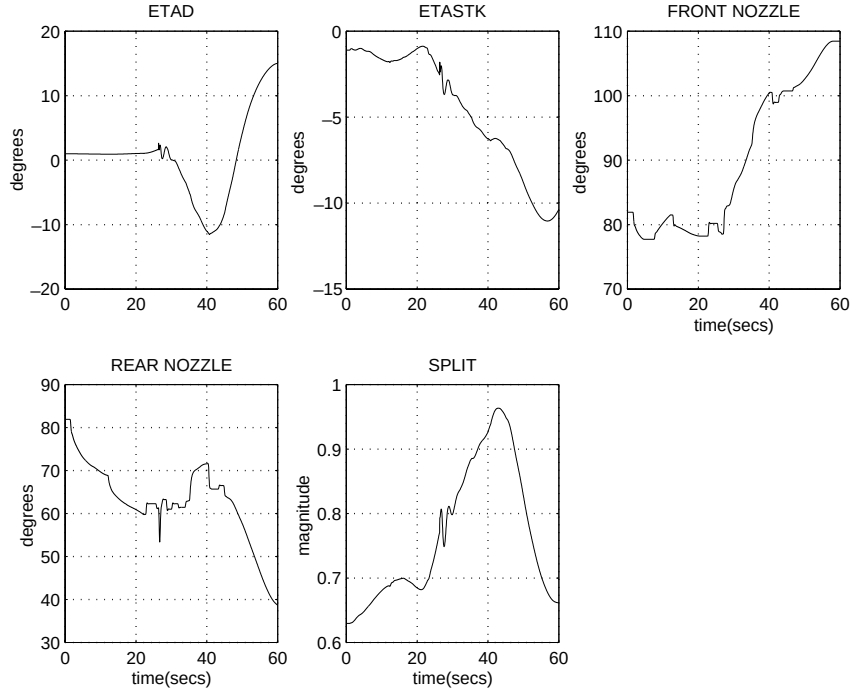

Fig. 5. Airframe actuator responses for pilot demands on VT in the acceleration from hover.

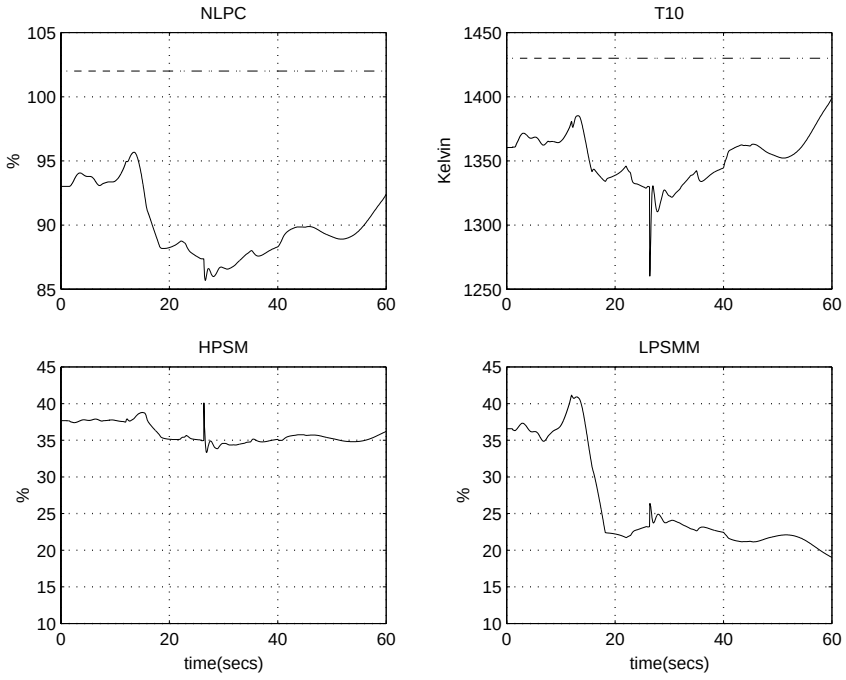

Fig. 6. Engine variable responses for pilot demands on VT in the acceleration from hover.

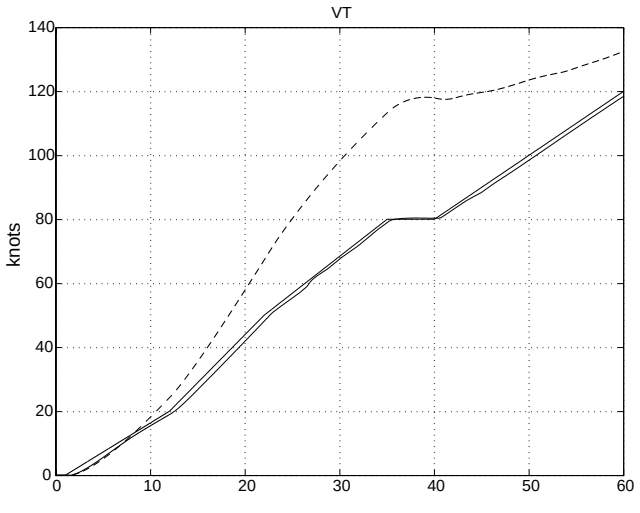

Fig. 7. Comparison of VT responses to pilot demands, scheduled IFPC system (–), single controller designed at hover (- -).

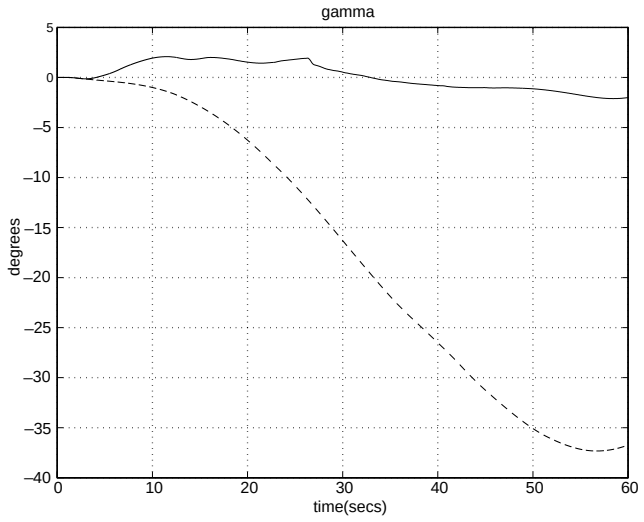

Fig. 8. Comparison of γ coupling for pilot demands on VT, scheduled IFPC system (–), single controller designed at hover (- -).

scheduled IFPC system with a single controller designed at the hover operating condition. As seen from the figures, the hover controller, which gives good performance at low speeds, is unable to cope with the large changes in the aircraft dynamics as it accelerates to wingborne flight.

5. A control signal blending approach

The approach to scheduling of $\mathscr{H}_\infty$ loopshaping controllers described above requires controllers at different operating points in the flight envelope to have the same state-space structure. A drawback of this requirement is that standard controller order reduction techniques (Glover, 1984) cannot be used to reduce the order of each controller prior to scheduling, as this will destroy the consistency of the state-space structure across different designs. This issue is of particular concern for the IFPC problem considered here, which, due to the complexity of the airframe/engine model, results (initially) in high-order controllers at each operating point. Initial attempts at order reduction

suggested, however, that these fixed-point controllers could be significantly reduced in order without any change in their closed-loop behaviour.

One solution to the above problem would be to try to reduce the order of each controller using techniques which preserve the physical interpretation of the state variables, see for example the approach described for an aero-engine control design in Harefors (1999). In general, such techniques are not well developed, however, and so in this study we opted to investigate a second method for scheduling the fixed-point controllers which imposes no constraints on the controllers' structure or order.

In this approach, the $\mathscr{H}_\infty$ loopshaping controllers are kept in their observer form as this structure was seen to provide slightly improved time-domain responses when compared with the implementation structure used in the piloted simulation trials (Fig. 1). The main idea of the proposed method is to interpolate the control signals produced by the different controllers, rather than interpolating the parameters of the controllers themselves. Writing the ith fixed-point controller as

$$\dot{\hat{x}}_s^i = A_s^i \hat{x}_s^i + H_s^i(C_s^i \hat{x}_s^i - y_s^i) + B_s^i u_s^i, \tag{25}$$

$$u_s^i = K_s^i \hat{x}_s^i, \tag{26}$$

the scheduled controller output is calculated in real time along the region between two design points i and $i+1$ as

$$u_s = (1-\lambda)u_s^i + \lambda u_s^{i+1},$$

where u_s^i is the output of the ith controller and u_s^{i+1} is the output of the $(i+1)$th controller. The interpolation factor λ is given by

$$\lambda = \frac{VT - VT^i}{VT^{i+1} - VT^i}, \quad i \in [0, 1],$$

where VT, VT^i and VT^{i+1} are the current velocity, velocity at the ith design point and the velocity at the $(i+1)$th design point, respectively. The structure of the blended IFPC system is shown in Fig. 9. Note that the blending of the control signals is done at the input of the shaped plant—the weighting functions for the plant were then interpolated in the same way as for the previous scheduling scheme. This was seen to give better performance than direct blending of the control signals at the plant input.

A significant advantage of this approach is that no requirements are placed on the structure or order of the different fixed-point controllers—in fact, they could even be designed using different synthesis methods. This structural freedom was exploited to reduce the order of each individual controller as much as possible without sacrificing performance or robustness properties. With respect to the observer form structure chosen to implement the $\mathscr{H}_\infty$ loopshaping controllers, the order of the shaped plant for each design given by

$$G_s^i = \left[\begin{array}{c|c} A_s^i & B_s^i \\ \hline C_s^i & 0 \end{array}\right]$$

was reduced to the lowest-order shaped plant

$$G_{sr}^i = \left[\begin{array}{c|c} A_{sr}^i & B_{sr}^i \\ \hline C_{sr}^i & 0 \end{array}\right]$$

such that $\|G_s^i - G_{sr}^i\|_\infty \leqslant tol$. The controller gains were then calculated for each reduced-order shaped plant G_{sr}^i. Note that all the shaped plants contain unstable states. Therefore, the shaped plants were first of all decomposed into stable and unstable parts—only the stable parts were used for order reduction, while the unstable states were added again at the end of the procedure. Using this approach, the order of each fixed-point controller could be significantly reduced using optimal Hankel norm order reduction techniques (Glover, 1984)

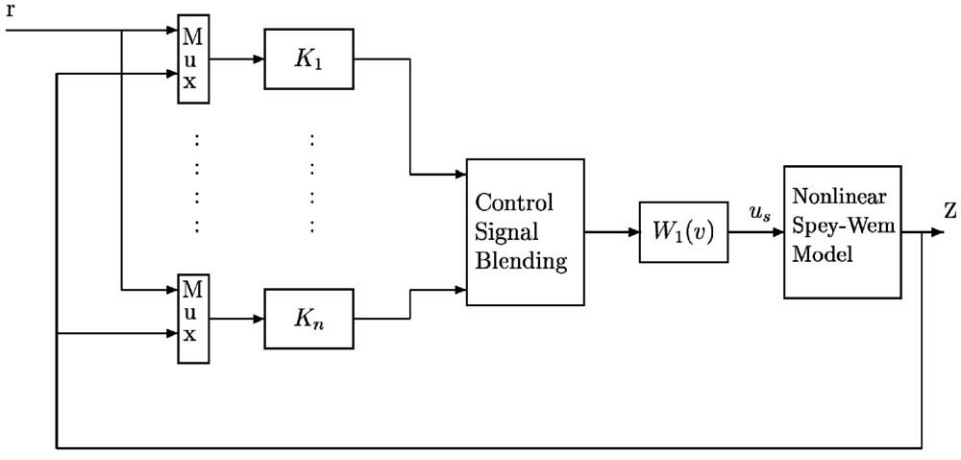

Fig. 9. Implementation of controller blending scheme.

with no significant change in closed-loop performance or robustness properties. Depending on the point in the envelope, final fixed-point controllers of order 14–19 were obtained.

Sample non-linear simulation results for the blended reduced-order IFPC system are shown in Figs. 10–12, for an acceleration from 20 to 120 kn. The figures show excellent tracking of velocity demands with minimal coupling into γ and α. In addition, all internal engine variables are held within their specified safety limits. Extending the schedule to include the hover flight condition resulted in slightly increased coupling into γ

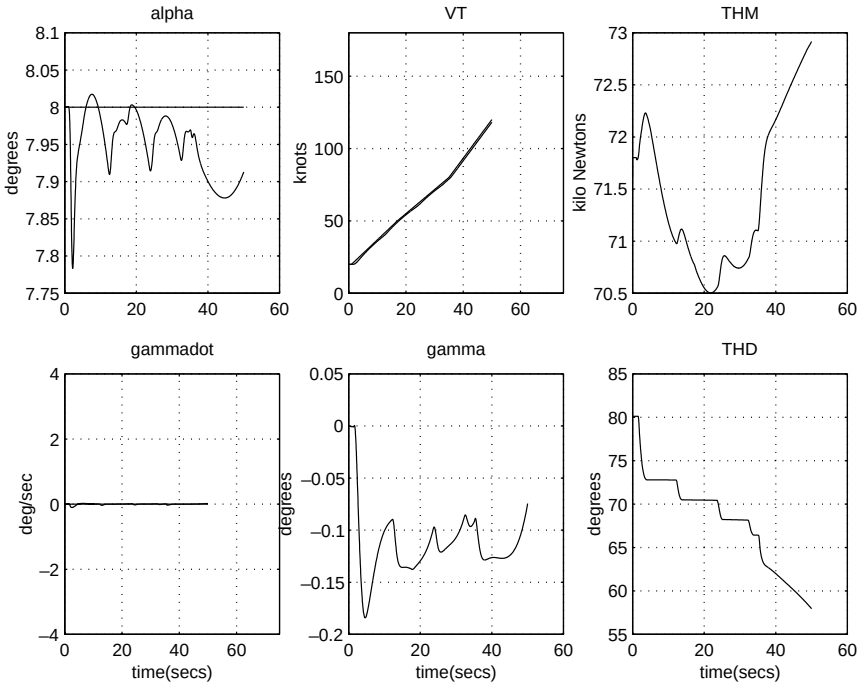

Fig. 10. Response of blended IFPC system for pilot demands on VT in the acceleration from 20 kn.

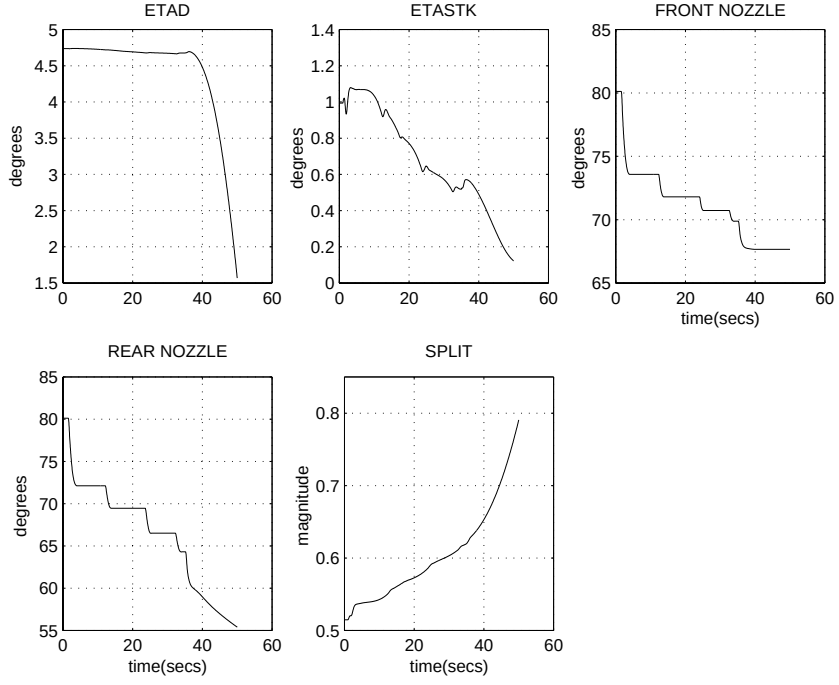

Fig. 11. Airframe actuator responses for pilot demands on VT in the acceleration from 20 kn.

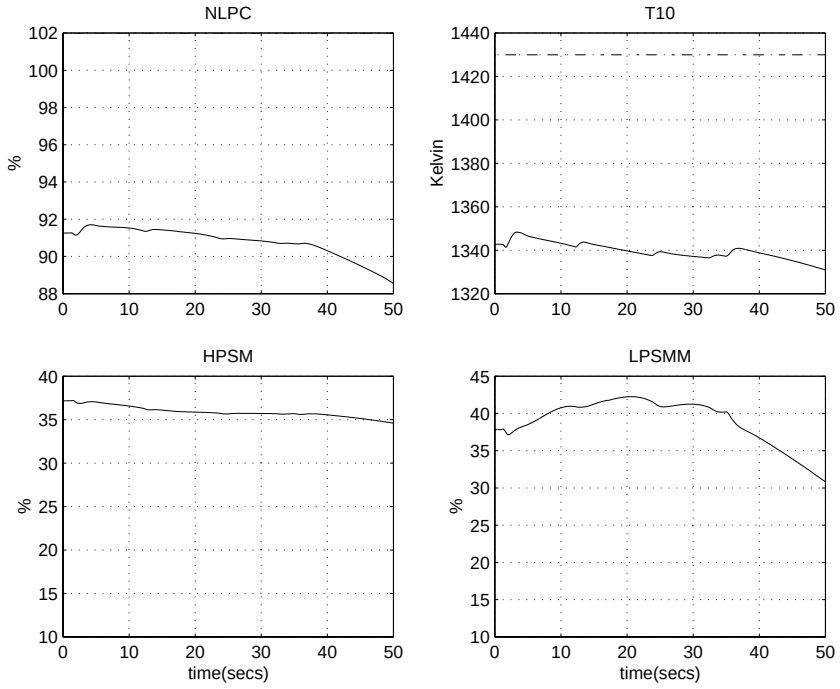

Fig. 12. Engine variable responses for pilot demands on VT in the acceleration from 20 kn.

due to the large variations in the aircraft dynamics between 0 and 20 kn. Overall, however, equivalent flying qualities were produced compared to those achieved with the observer-form scheduling scheme, in spite of the fact that the order of the individual fixed-point controllers was reduced significantly.

Although no stability problems were encountered in non-linear simulation for either of the scheduling schemes described above, no a priori guarantees are generally provided by interpolation or blending methods that the resulting scheduled controller will provide closed-loop stability for the real non-linear system. Recent work on stability-preserving interpolation methods (Stilwell & Rugh, 2000; Stilwell, 2001) has shown that 'theoretically justified' scheduling schemes can be developed which are guaranteed to be at least locally stabilising at every operating point of the non-linear plant. We note, however, that the stability guarantees provided by these methods apply only to an LPV representation of the non-linear plant, and the weighting functions used in the interpolation depend on the solution of computationally expensive LMI-based optimisation problems.

Finally, an important issue in the design of IFPC systems for V/STOL aircraft is the requirement for decentralised or partitioned low-order implementations of the overall integrated control system (Gatley, Bates, & Postlethwaite, 2000). The application of the scheduling schemes described in this paper to a partitioned IFPC system is the subject of current research by the authors.

6. Conclusions

This paper has considered two approaches to the design of a scheduled integrated flight and propulsion control system for an experimental V/STOL aircraft concept in the acceleration from hover flight phase. Integrated flight and propulsion controllers were designed at several points over the V/STOL envelope from hover to 120 kn using the method of $\mathscr{H}_\infty$ loopshaping. These controllers were then implemented as plant observers with state feedback. In the first approach, the observer/controller gain matrices were scheduled via interpolation as a function of aircraft speed. The resulting scheduled IFPC system was shown in non-linear simulation to provide excellent handling qualities as the aircraft accelerates from hover, while also keeping safety-limited engine variables within specified limits. Problems with using standard controller order reduction methods under this scheduling framework were highlighted. This issue motivated a second scheduling strategy based on a blending of the control signals entering the shaped plant. This scheme was seen to allow for significant reduction in the orders of the individual controllers, while maintaining level 1 type handling

qualities over the considered region of the V/STOL flight envelope.

References

Aouf, N., Bates, D. G., & Postlethwaite, I. (2001). Observer-form scheduling of a $\mathscr{H}_\infty$ loopshaping integrated flight and propulsion control law. *Proceedings of the AIAA conference on guidance, navigation and control*, AIAA-01-4388.

Bates, D. G., Gatley, S. L., Postlethwaite, I., & Berry, A. J. (1999). Integrated flight and propulsion control system design using $\mathscr{H}_\infty$ loopshaping techniques. *Proceedings of the IEEE conference on decision and control* (pp. 1523–1528).

Bates, D. G., Gatley, S. L., Postlethwaite, I., & Berry, A. J. (2000). Design and piloted simulation of a robust integrated flight and propulsion controller. *AIAA Journal of Guidance, Control and Dynamics*, *23*(2), 269–277.

Buschek, H. (1999). Full envelope missile autopilot design using gain scheduled robust control. *AIAA Journal of Guidance, Control and Dynamics*, *22*(1), 115–123.

Cooper, G. E., & Harper Jr., R. P. (1969). The use of pilot rating in the evaluation of aircraft handling qualities. NASA TN D-5153.

Doyle, J. C., Glover, K., Khargoneker, P. P., & Francis, B. A. (1989). State-space solutions to standard $\mathscr{H}_2$ and $\mathscr{H}_\infty$ control problems. *IEEE Transactions on Automatic Control*, *AC-34*(8), 831–847.

Garg, S. (1993a). Robust integrated flight/propulsion control design for a STOVL aircraft using $\mathscr{H}_\infty$ control design techniques. *Automatica*, *29*(1), 129–145.

Garg, S. (1993b). Partitioning of centralised integrated flight/propulsion control design for decentralised implementation. *IEEE Transactions on Control Systems Technology*, *1*(2), 93–100.

Gatley, S. L., Bates, D. G., & Postlethwaite, I. (2000). A partitioned integrated flight and propulsion control system with engine safety limiting. *Control Engineering Practice*, *8*(8), 845–860.

Glover, K. (1984). All optimal hankel norm approximations of linear multivariable systems and their $\mathscr{L}^\infty$ error bounds. *International Journal of Control*, *36*(9), 1115–1193.

Glover, K., Vinnicombe, G., & Papageorgiou, G. (2000). Guaranteed multi-loop stability margins and the gap metric. *Proceedings of the IEEE conference on decision and control*, Sydney.

Harefors, M. (1999). A study in jet engine control—control structure selection and multivariable design. Ph.D. Thesis, Chalmers University of Technology, Sweden.

Hyde, R. A. (1995). *$\mathscr{H}_\infty$ Aerospace control design—a VSTOL flight application*. Berlin: Springer.

McFarlane, D., & Glover, K. (1992). A loop shaping design procedure using $\mathscr{H}_\infty$ synthesis. *IEEE Transactions on Automatic Control*, *AC-36*, 759–769.

Papageorgiou, G., & Glover, K. (1999). $\mathscr{H}_\infty$ Loop shaping: Why is it a sensible procedure for designing robust flight controllers? In *Proceedings of the AIAA conference on guidance, navigation and control*, Oregon, AIAA-99-4272.

Papageorgiou, G., & Glover, K. (2000). Development of a 'reliable' LPV model for the longitudinal dynamics of DERA's VAAC Harrier. *Proceedings of the AIAA conference on guidance, navigation and control*, AIAA-00-4450.

Papageorgiou, G., Glover, K., D'Mello, G., & Patel, Y. (2000). Taking robust LPV control into flight on the VAAC harrier. *Proceedings of the IEEE Conference on Decision and Control*, Sydney.

Ran, A. C., & Rodman, L. (1988). On parameter dependence of solutions of algebraic Riccati equations. *Mathematics of Control, Signals and Systems*, (1), 269–284.

Schmidt, D. K. (1993). Integrated control of hypersonic vehicles—a necessity not just a possibility. AIAA-93-3761-CP.

Sefton, J. A., & Glover, K. (1990). Pole/zero cancellations in the general $\mathscr{H}_\infty$ problem with reference to a two block design. *Systems and Control Letters*, *14*, 295–306.

Shamma, J. S., & Cloutier, J. R. (1993). Gain-scheduled missile autopilot design using linear parameter varying transformations. *AIAA Journal of Guidance, Control and Dynamics*, 256–263.

Skogestad, S., & Postlethwaite, I. (1996). *Multivariable feedback control*. New York: Wiley.

Steer, A. J. (2000). Integrated control of a second generation supersonic commercial transport aircraft using thrust vectoring. *Proceedings of the AIAA conference on guidance, navigation and control*, AIAA paper No. 2000-4109.

Stevens, B. L., & Lewis, F. L. (1992). *Aircraft simulation and control*. New York: Wiley.

Stilwell, D. (2001). State-space interpolation for a gain scheduled autopilot. *AIAA Journal of Guidance, Control and Dynamics*, *24*(3), 460–465.

Stilwell, D., & Rugh, W. R. (2000). Interpolation methods for the synthesis of gain scheduled controllers. *Automatica*, *36*(5), 665–671.

Tischler, M. B. (Ed) (1996). *Advances in aircraft flight control*, London: Taylor and Francis (Chapter 6).

Wise, K. A. (1995). Applied controls research topics in the aerospace industry. *Proceedings of the IEEE conference on decision and control* (pp. 751–756).